Inorganic Chemistry

Article

pubs.acs.org/IC

Chlorine-35 Solid-State NMR Spectroscopy as an Indirect Probe of Germanium Oxidation State and Coordination Environment in Germanium Chlorides

Margaret A. Hanson,[†] Victor V. Terskikh,[‡] Kim M. Baines,*[,†] and Yining Huang*[,†]

[†]Department of Chemistry, The University of Western Ontario, London, Ontario, Canada N6A 5B7

[‡]Department of Chemistry, University of Ottawa, Ottawa, Ontario, Canada K1N 6N5

Supporting Information

ABSTRACT: Due to the prevalence of Ge−Cl bonds in germanium chemistry and the inherent challenges of germanium-73 NMR spectroscopy, chlorine-35 NMR spectroscopy was investigated as an indirect method of characterization for these ubiquitous and useful compounds. Chlorine-35 NMR parameters were correlated with structural metrics as well as the oxidation state of germanium.

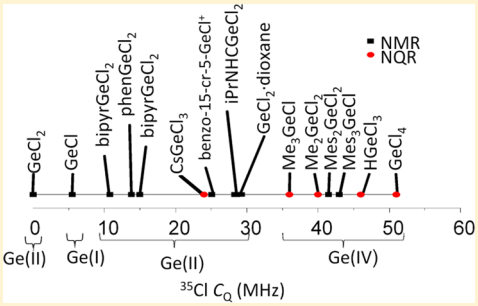

INTRODUCTION

Germanium chlorides are a fundamentally important class of compounds. $GeCl_4$ and $GeCl_2$·dioxane are useful, convenient, and ubiquitous starting materials for the synthesis of germanium(IV) and germanium(II) compounds,[1] respectively. In recent years, a wealth of unprecedented stable low valent[2−5] and cationic[4,6] germanium complexes have been synthesized, most of which are made starting from a germanium chloride and many retain an interaction between germanium and the halogen.[7] Given the prevalence and importance of germanium chlorides, it is important to have an understanding of the electronic structure at the reactive center including the oxidation state[1] of germanium; however, methods for the determination of the oxidation state of germanium are not readily available, and furthermore, the oxidation state of the heavier group 14 elements is not always readily assigned.[8]

Thus far, the most useful tool for the characterization of low valent and cationic germanium halides has been X-ray crystallography. However, accurate crystallographic characterization requires high quality single crystals of a suitable size, which can be very challenging to grow. Additionally, crystallography provides insight into the coordination environment, but not the electronic structure of the molecule.[1] While Mössbauer spectroscopy can be used to assess oxidation states, it is only commonly employed for iron, tin, antimony, and iodine, while many other elements, germanium included, lack an appropriate gamma ray source.[9] A useful tool for assessing oxidation states is a synchrotron technique, X-ray Absorption Near Edge Structure (XANES).[10] While XANES is feasible for main group compounds,[11] a more readily accessible methodology is desirable.

It is increasingly possible to obtain structural and electronic information from powder samples by solid-state NMR (SSNMR) spectroscopy.[12] The quadrupolar parameters of ^{93}Nb have previously been shown to be sensitive to the oxidation state of the niobium center, with niobium(V) compounds exhibiting larger C_Q[^{93}Nb] values than niobium(I).[13] Additionally, a relationship was observed between the oxidation state of metals in the second coordination sphere of octahedral niobates and the CSA [^{93}Nb] tensor.[14] Niobium is a nucleus for which Mössbauer spectroscopy is not available, and thus, oxidation states are generally assessed by X-ray photoelectron spectroscopy (X-ray PES).[15]

A major obstacle to the application of SSNMR spectroscopy for the characterization of germanium compounds is the unfavorable NMR properties of ^{73}Ge. While its homologues ^{13}C, ^{29}Si, ^{119}Sn, and ^{207}Pb, all with a spin of 1/2, are relatively routine nuclei for NMR spectroscopy, germanium possesses considerably less favorable NMR properties. ^{73}Ge, the only NMR active isotope of germanium, is quadrupolar with a spin of 9/2 and has a moderate quadrupole moment of −19.6 mb.[16] ^{73}Ge also has a low natural abundance (7.76%); however, the greatest challenge is that ^{73}Ge has one of the smallest gyromagnetic ratios in the periodic table, corresponding to a Larmor frequency of only 31.4 MHz at 21.1 T (900 MHz for ^{1}H).[17]

While ^{73}Ge is a challenging nucleus, higher field instruments, which offer a more favorable Boltzmann distribution as well as diminished broadening from the second order quadrupolar interaction, and new sensitivity-enhancement pulse sequences[18] have made ^{73}Ge NMR spectroscopy accessible under favorable conditions of either high symmetry[19] at germanium or high (>4 Ge atoms/1000 Å^3)[20] germanium content in the sample.[21] However, perfect spherical symmetry at germanium is not common.

Received: March 28, 2014
Published: June 20, 2014

   dx.doi.org/10.1021/ic500728w | Inorg. Chem. 2014, 53, 7377−7388

Furthermore, many interesting germanium compounds are kinetically stabilized by bulky ligands, and as a consequence, the overall germanium content in a given volume is low. Lower concentrations of germanium in the unit cell lead to lower signal-to-noise ratios, much like in solution. As a result, it has not been possible to obtain sufficient data to determine whether there is a relationship between ^{73}Ge NMR parameters and the oxidation state of germanium.

Due to the prevalence of Ge−Cl bonds in germanium chemistry, we are interested in exploring solid-state ^{35}Cl NMR spectroscopy as an indirect method for obtaining information about germanium. Using spectra of an attached atom is not unprecedented, for example, ^{31}P J-coupling constants have been shown to be related to rhodium oxidation states.[22] Phosphorus has also been used to provide additional information about quadrupolar nuclei.[23] To assess chlorine as a potential source of information, we chose to undertake a systematic investigation of various compounds containing Ge−Cl bonds to determine what information about the germanium oxidation state and coordination environment might be determined from the ^{35}Cl NMR parameters. To fully examine the scope of the technique, we included examples of both germanium(II) and the more common germanium(IV) compounds

There are two NMR active isotopes of chlorine: ^{35}Cl and ^{37}Cl. Both are quadrupolar with a spin of 3/2 and have large quadrupole moments (Q = −81.65 mb for ^{35}Cl, −64.35 mb for ^{37}Cl),[16] which results in extremely broad NMR signals in the absence of spherical symmetry.[24] Both isotopes are considered to be low gamma with Larmor frequencies of 88.19 MHz (^{35}Cl) and 73.41 MHz (^{37}Cl) at 21.1 T. Due to the much higher natural abundance of ^{35}Cl (75% versus 25% for ^{37}Cl), it is generally the preferred isotope for NMR spectroscopy; however, ^{37}Cl studies are also feasible and are sometimes used as a method of verifying ^{35}Cl parameters. Extremely broad quadrupole NMR spectra are much more easily acquired at ultrahigh (>18.8 T) magnetic field due to the inverse relationship between the second order quadrupolar broadening and the magnetic field strength. Additionally, the study of these nuclei has benefited greatly from the use of Quadrupolar Carr Purcell Meiboom Gill (QCPMG)[25] and related pulse sequences.[26−28] In the QCPMG sequence, a 90° pulse is followed by a 180° refocusing pulse, as in the standard spin−echo experiment. Rather than allowing the magnetization to decay normally, it is instead repeatedly refocused by a series of 180° pulses. When the echo train is Fourier transformed, the broad signal is collected into a series of spikelets, leading to an improved signal-to-noise ratio. Due to the extreme breadth of typical ^{35}Cl NMR spectra, it is often necessary to acquire multiple subspectra at evenly spaced transmitter frequencies which are then added together to give the total spectrum. Recently introduced adiabatic Wideband Uniform Rate Smooth Truncation (WURST) pulses have greatly improved the excitation profile of the QCPMG sequence.[29] While stepwise spectral acquisition is often still required, the overall number of subspectra required is greatly reduced, thereby considerably shortening the total acquisition time.

Several recent reviews on ^{35}Cl NMR spectroscopy have been published.[30−32] Through a combination of stepwise acquisition and the WURST-QCPMG pulse sequence, it has become increasingly feasible to study chlorine in a covalent environment in addition to simple ionic inorganic chlorides. Recently, a series of chloride substituted group IV transition metal catalysts was examined.[33] Through the use of ^{35}Cl SSNMR spectroscopy and DFT calculations, a structure was proposed for Schwartz's reagent, an important catalyst for which X-ray quality single crystals had not been obtained. Particularly notable is an investigation of organic chlorides featuring chlorine covalently bound to carbon, which have the largest quadrupolar coupling constants observed by NMR spectroscopy to date (C_Q [^{35}Cl] = 66−75 MHz).[34] Uncomplexed $GeCl_2$ has also been studied by ^{35}Cl SSNMR spectroscopy.[35] A single narrow signal was observed under static conditions with an estimated C_Q of less than 40 kHz. The crystal structure of $GeCl_2$ is unknown and had previously been proposed to be similar in structure to the distorted octahedral $GeBr_2$.[36] However, the combined ^{35}Cl and ^{73}Ge SSNMR data suggest a structure similar to the regularly octahedral GeI_2, with high symmetry at both germanium and chlorine and a single halogen site. This illustrates the potential utility of ^{35}Cl SSNMR spectroscopy in probing the coordination environment of germanium.

In comparison to the relatively few examples of ^{35}Cl NMR spectroscopic studies of group 14 chlorides, there have been a considerable number of investigations of germanium chlorides by nuclear quadrupole resonance (NQR) spectroscopy.[37] These investigations have largely focused on compounds with germanium in the higher oxidation state due to the prevalence of germanium(IV) compounds compared to germanium(II) compounds. At the time of these studies, there were very few stable compounds with germanium in the +2 oxidation state. A particularly notable study used *ab initio* calculations of NQR frequencies to relate the quadrupolar frequency to the Ge−O bond length.[38] A considerable advantage of NMR spectroscopy over NQR is the ability to directly measure the value of η_Q, which provides additional information about the symmetry around chlorine.

In this study, we focus on a variety of low valent germanium chlorides stabilized by a donor and shown in Figure 1. Solid-state

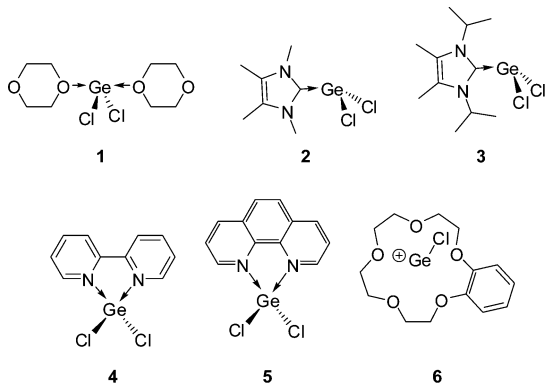

Figure 1. Germanium(II) complexes examined in this study.

NMR parameters are strongly influenced by structure, and thus, the most prominent structural features of the germanium chlorides **1**−**6** are reviewed here.

While $GeCl_2$ is a nominally stable germylene, it is only isolated in polymeric form.[39] A more convenient starting material for the synthesis of germanium(II) compounds is germanium dichloride complexed with dioxane ($GeCl_2$·dioxane, **1**).[40] This complex is readily synthesized from $GeCl_4$ and is stable under inert conditions.[6] $GeCl_2$·dioxane is a coordination polymer composed of infinite chains of alternating $GeCl_2$ and dioxane units.[41] There is one crystallographically unique germanium site (C_2 symmetry) and one unique chlorine site (C_s symmetry). The germanium atom has two strong covalent bonds to chlorine atoms (Ge−Cl bond

dx.doi.org/10.1021/ic500728w | *Inorg. Chem.* 2014, 53, 7377−7388

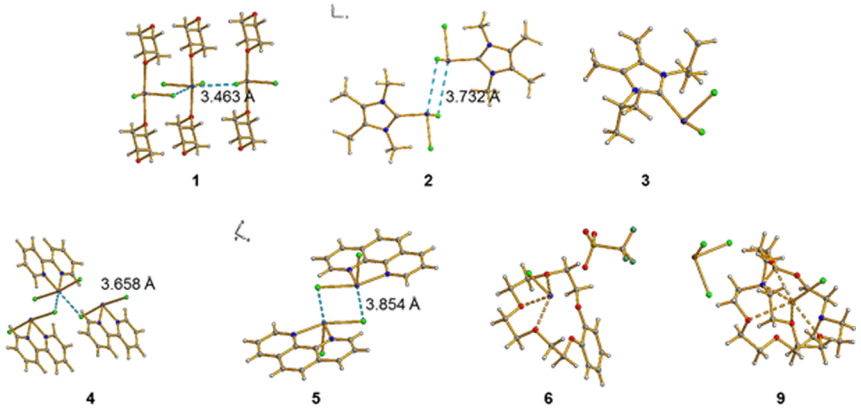

Figure 2. X-ray structures of compounds **1**−**6** and **9** showing the long-range interactions between chlorine (green) and germanium (purple) in **1**, **2**, **4**, and **5**.

length = 2.281 Å) and two weak bonds to the oxygen of the dioxane (Ge−O distance = 2.3999 Å; a typical Ge−O bond length falls in the range of 1.75−1.85 Å[42]). Additionally, there are two nonbonded chlorides found at a distance of 3.463 Å from the adjacent Ge, resulting in an overall pseudo-octahedral geometry at germanium and a pseudobridging environment for chlorine (Figure 2).

Two N-heterocyclic carbene (NHC) complexes of $GeCl_2$ (**2**[43] and **3** (iPrNHC$GeCl_2$)[44]) were also included in the investigation. Complex **2**, with methyl groups on the nitrogen of the NHC ligand, features a long-range (3.732 Å) interaction between the chloride of one complex and the germanium of the adjacent molecule (Figure 2). With larger isopropyl groups on nitrogen, as in complex **3**, the molecules are not in close enough proximity to each other for a chloride to interact with the germanium of an adjacent complex (shortest $Ge_{(adjacent)}$−Cl distance > 6.9 Å), leading to a truly terminal environment for the chloride.

Two $GeCl_2$ complexes with neutral nitrogen donors, 2,2′-bipyridine (**4**; bipyr$GeCl_2$) and 1,10-phenanthroline (**5**), were also investigated. The bipyridine complex **4** resembles $GeCl_2$·dioxane in that a long-range Ge−Cl contact (3.658 Å) leads to a pseudooctahedral environment at germanium.[7f] Unlike $GeCl_2$·dioxane, the covalent Ge−Cl bonds in the bipyridine complex are of different lengths (Ge−Cl(1) = 2.5428 Å and Ge−Cl(2) = 2.7195 Å) leading to two crystallographically distinct chlorine sites. In contrast, the phenanthroline complex **5** (phen$GeCl_2$) is a weakly associated centrosymmetric dimer with one terminal chloride site (Ge−Cl = 2.3145 Å) and the other chloride (Ge−Cl = 2.6276 Å) forming a weak bridging interaction (Figure 2).[7f]

A cationic germanium(II) complex stabilized by benzo-15-crown-5 (**6**; benzo-15-cr-5-$GeCl^+$) was also included in this study.[45] In this case, the single chloride is in a terminal position, with a Ge−Cl bond length of 2.288 Å and no interaction with the adjacent ions. While a series of cationic crown ether complexes is known,[45,46] the benzo-15-crown-5 derivative was specifically selected for this study because the counterion is triflate rather than $GeCl_3^-$, simplifying the expected ^{35}Cl NMR spectrum.

As the +4 oxidation state is far more common in germanium chemistry, two prototypical germanium(IV) chlorides were also investigated (Figure 3). The two related compounds, dichlorodimesitylgermane (**7**) and chlorotrimesitylgermane (**8**), are, given the large size of the mesityl group, believed to feature chlorine in a terminal environment as is typical in germanium(IV) chemistry.[42] Neither of these compounds have a known crystal structure.

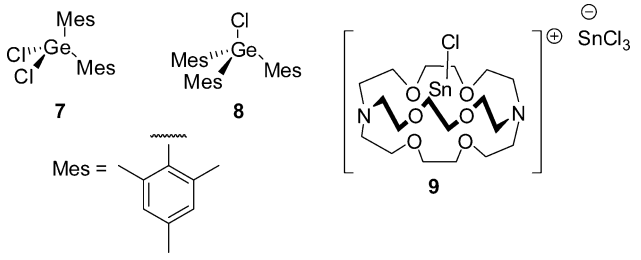

Figure 3. Additional compounds examined in this study.

To complement the Ge−Cl study, a cationic cryptand complex of tin chloride (**9**)[47] was included (Figure 3). While a cryptand is used instead of a crown ether, **9** is, in general terms, quite similar to **6**: a macrocyclic ether is used to stabilize a reactive group 14 cation in the +2 oxidation state. As would be expected for a larger atom, the Sn−Cl bond length (2.532 Å) is notably longer than what was observed for the germanium cation.

RESULTS

Solid-State NMR Spectroscopy. Attempts were made to obtain ^{73}Ge spectra for compounds **1**−**5** and **7**, but only the spectrum of **1** was successfully acquired.[48] $GeCl_2$·dioxane has a very high germanium concentration, making it possible to obtain a spectrum with a reasonable signal-to-noise ratio despite the large C_Q value leading to a broad signal. The ligands in **2**−**5** and **7** are much bulkier than dioxane, leading to a lower overall germanium content in the unit cell. Additionally, in some cases the quadrupolar chlorines may result in short T_2 relaxation times. Since the QCPMG signal enhancement comes in part from the ability to refocus the signal repeatedly before decay, a short T_2 leads to minimal benefit. As direct observation of the germanium center was not a feasible method of characterization for compounds **2**−**8**, we investigated ^{35}Cl SSNMR spectroscopy as an alternate means of characterization.

A summary of the experimental ^{35}Cl NMR results is presented in Table 1. The ^{35}Cl SSNMR spectra of complexed germylenes **1**−**6** differed considerably from that of uncomplexed $GeCl_2$.[35] While $GeCl_2$ gave rise to remarkably narrow lines, the signals in this study are more typical of covalent chlorides with pronounced quadrupolar lineshapes. Clearly, the environment around germanium has an impact on the ^{35}Cl NMR parameters, particularly in cases where there is a strongly bound electron donor altering the symmetry at germanium.

dx.doi.org/10.1021/ic500728w | Inorg. Chem. 2014, 53, 7377−7388

Table 1. Summary of Experimental ^{35}Cl NMR Parameters from Static NMR Spectra Acquired at 21.1 T

compound	δ_{iso} (ppm)	C_Q [^{35}Cl] (MHz)	η_Q	Ω (ppm)	κ^a
1	300(50)	28.3(1)	0.055(10)	250(100)	1
2	200(50)	29.3(1)	0.12(2)	300(100)	1
3	150(50)	28.6(3)	0.23(5)	n.o.[b]	n.o.[b]
4	200(50)	15.3(1)	0.13(2)	n.o.[b]	n.o.[b]
	250(50)	14.1(1)	0.10(2)	250(100)	0
5	250(50)	13.8(1)	0.15(2)	200(100)	0
	250(50)	29.6(1)	0.18(2)	n.o.[b]	n.o.[b]
6	300(50)	25.1(1)	0.10(2)	350(100)	1
7	200(100)	43.0(5)	0.1(1)	n.o.[b]	n.o.[b]
8	200(100)	41.5(5)	0	n.o.[b]	n.o.[b]
9	200(50)	19.0(1)	0.15(5)	n.o.[b]	n.o.[b]

[a]Euler angles were set to $\alpha = \beta = \gamma = 0$ due to the small effect of CSA. [b]n.o. = not observed.

The ^{35}Cl SSNMR spectrum of **1** provides an excellent illustration of the advantages of the WURST-QCPMG pulse sequence over the simple QCPMG sequence. The QCPMG spectrum of **1** (Figure 4A) required the acquisition of 13 individual subspectra at 100 kHz offset over a total of 9 h. The use of the WURST-QCPMG sequence (Figure 4B) reduced the number of subspectra required to two and the total acquisition time to 45 min. Additionally, the overall line shape of the coadded spectrum was much smoother using the WURST-QCPMG spectrum, making the central discontinuity easier to detect and thus increasing the accuracy of the ^{35}Cl NMR parameters extracted from analytical simulations.

Although the interaction between the electric field gradient (EFG) and the quadrupole moment of the chlorine nucleus is the dominant interaction for ^{35}Cl, it was not possible to accurately reproduce the position of the central discontinuity of the spectrum of $GeCl_2$·dioxane without including chemical shielding anisotropy (CSA; Figure 4B). Proper positioning of the central discontinuity of the spectrum required a span of approximately 250 ppm ($\kappa = 1$). Due to the small effect of the CSA on the spectrum, Euler angles were all left at zero, although there is no symmetry element requiring this. The quadrupolar coupling constant of 28.3 MHz is consistent with the low symmetry environment around chlorine[41] and falls within the range observed for group 13 chlorides[49] and well below the values determined for organic chlorides containing covalent C−Cl bonds.[34] The quadrupolar asymmetry parameter ($\eta_Q = 0.055$) corresponds to an essentially axially symmetric environment despite the fact that there is not a C_3 or higher axis through the Ge−Cl bond. Terminal chlorides tend to have small (<0.2) η_Q values even in the absence of axial symmetry, while bridging chlorides tend to have larger η_Q values,[33,50] suggesting that the long-range pseudobridging interaction observed in the X-ray structure of **1**[41] is not strong enough to disrupt the overall symmetry of the EFG tensor.

While the two NHC complexes of $GeCl_2$ (**2** and **3**) are extremely similar in structure as determined by X-ray crystallography,[43,44] the ^{35}Cl SSNMR spectra exhibit distinct differences (Figure 5). Complex **2** has a somewhat broader ^{35}Cl spectrum than $GeCl_2$·dioxane, with a C_Q [^{35}Cl] value of 29.3 MHz. To fit the spectrum of **2** acquired at 21.1 T accurately, a small amount of CSA interaction (Ω = 300 ppm) must be included. The parameters were verified by fitting the spectrum acquired at 9.4 T (Figure S1) with the same values. The sharp signal around 0 ppm in both spectra is likely the hydrochloride salt of the N-heterocyclic carbene arising as a decomposition product due to the air and moisture sensitivity of these compounds. The considerably poorer signal-to-noise ratio of **3** can be attributed to the shorter T_2 relaxation as estimated from the FID leading to decreased signal enhancement from the WURST-QCPMG pulse sequence. The rapid relaxation likely arises from crystal packing effects allowing greater mobility in the isopropyl groups when compared to the methyl groups in **2**. The spectrum of **3** was fit with C_Q [^{35}Cl] = 28.6 and η_Q = 0.23. Due to the poor signal-to-noise ratio, it was not possible to determine any contributions from CSA.

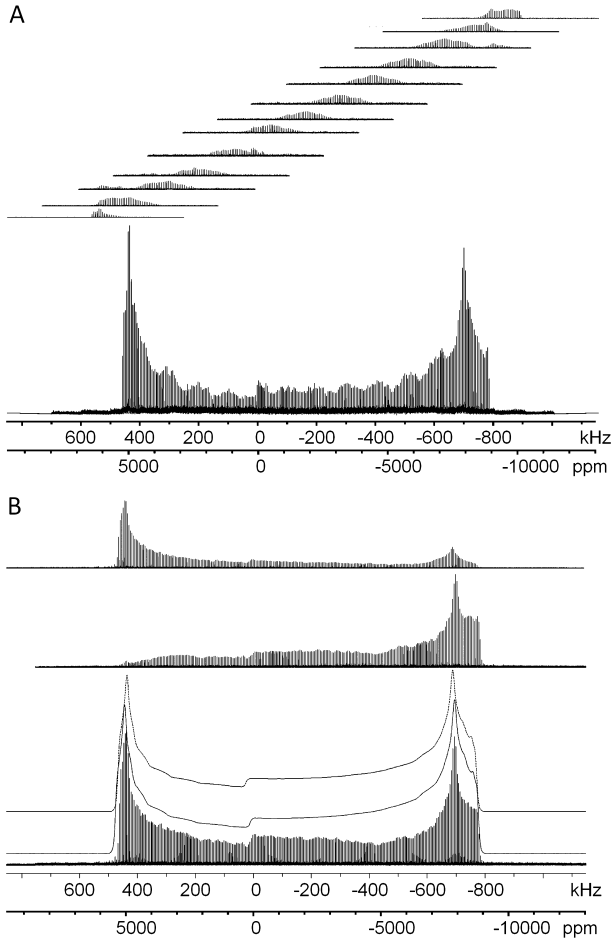

Figure 4. (A) Individual static ^{35}Cl QCPMG NMR subspectra (offset = 100 kHz) and coadded spectrum of $GeCl_2$·dioxane (**1**) at 21.1 T. (B) Individual static ^{35}Cl WURST-QCPMG subspectra (no offset, but opposite sweep directions) and coadded spectrum of $GeCl_2$·dioxane (**1**) at 21.1 T. The top trace indicates the empirical simulation accounting for only the EFG interaction. The bottom trace indicates the simulation including CSA.

The ^{35}Cl SSNMR spectrum of **4** (Figure 6) shows two distinct overlapping signals, one with C_Q [^{35}Cl] = 14.1 MHz and the other with C_Q [^{35}Cl] = 15.3 MHz. A WURST-Echo spectrum was acquired in addition to the WURST-QCPMG spectrum in order to resolve the high frequency discontinuities of the individual signals. Both signals have nonzero η_Q values (0.10 and 0.13, respectively) which suggest somewhat less than axial symmetry. A small CSA (Ω = 250 ppm) was required to fit the narrower signal, but the overlap of the two signals meant that the central discontinuity that has proven crucial for CSA determination in the other complexes was not visible for the broader signal in this spectrum. While both chlorides in **4** are found in similar

dx.doi.org/10.1021/ic500728w | Inorg. Chem. 2014, 53, 7377−7388

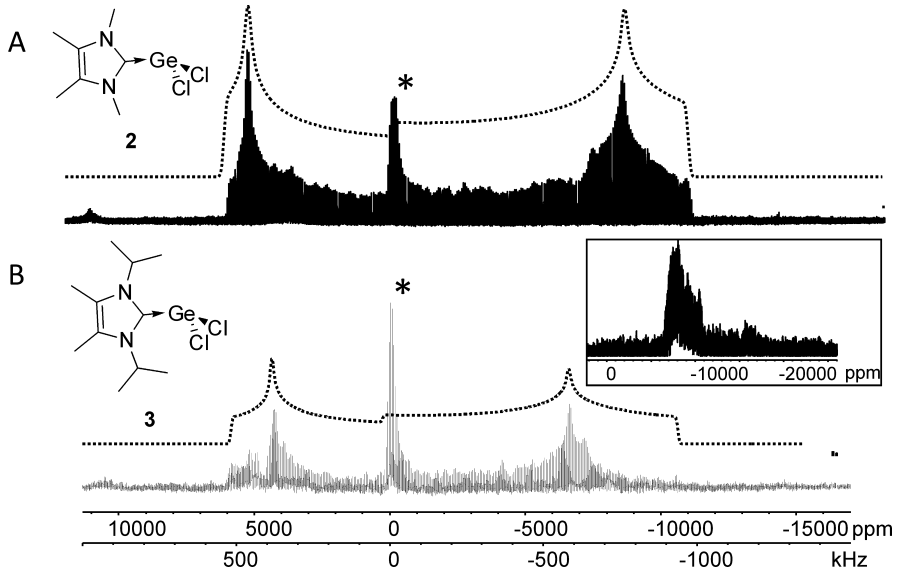

Figure 5. Static ^{35}Cl WURST-QCPMG NMR spectra of (A) **2** and (B) **3** at 21.1 T. Dotted traces indicate empirical simulations. An impurity of the hydrochloride salt of the carbene is indicated by an asterisk. The rightmost discontinuity in the spectrum of **3** was confirmed by an additional experiment with a longer acquisition time of 16 h (shown as inset, see Table S2 for experimental conditions).

pseudobridging environments, the Ge−Cl bond lengths differ by 0.3 Å,[7f] which leads to different EFG tensors, a difference which was also observed at 9.4 T (Figure S2). The resolution of the two signals is notable as it is uncommon (though not unprecedented[51]) to observe separate chlorine sites except in cases where one site is bridging and the other terminal. It is not clear from the spectrum alone which signal arises from which site, necessitating DFT calculations for further insight (*vide infra*).

The spectrum of the phenanthroline complex **5** consists of two overlapping signals. The narrower signal has C_Q [^{35}Cl] = 13.8 MHz, which is similar to the two C_Q [^{35}Cl] values determined for the bipyridine complex **4**. Much like complex **4**, the η_Q value of 0.15 suggests a slight deviation from axial symmetry. To accurately fit the central discontinuity of the narrow signal of complex **5** using the same parameters determined from the low field data (Figure S3), it was necessary to include a small (Ω = 200 ppm, κ = 0) CSA contribution. The second signal is considerably broader, with C_Q [^{35}Cl] = 29.6 MHz and η_Q = 0.18. The dramatic difference in C_Q values is readily explained by the fact that one chlorine site is weakly bridging while the other is terminal, although it is not possible to conclude from the data alone which site corresponds to which signal.

Consistent with the low symmetry of a terminal chloride, the ^{35}Cl SSNMR spectrum of [benzo-15-crown-5-GeCl][OTf], **6**, has a C_Q [^{35}Cl] of 25.1 MHz (Figure 7). To completely fit the line shape, it was necessary to include a CSA contribution comparable to others in this study (Ω = 350 ppm, κ = 1). A skew value indicative of axial symmetry was consistent with the near axial η_Q value (0.1). On the basis of the relatively small magnitude of the CSA in comparison to the EFG interaction, the error is quite large on the former.

The ^{35}Cl SSNMR spectrum of Mes_2GeCl_2 (**7**; Figure 8) differed considerably from the spectra of the germanium(II) compounds. The signal was considerably broader, spanning approximately three megahertz at 21.1 T. The quadrupolar coupling constant of 43 MHz was the largest observed in this study, though larger are known.[24,34,52] The ^{35}Cl SSNMR spectrum of Mes_3GeCl (**8**) exhibited similar features, with a C_Q [^{35}Cl] value of 41.5 MHz. Notably, organic chlorides, for which all published data concerns carbon(IV), exhibit C_Q values even larger than those observed for the germanium(IV) compounds.[34] While there are no other ^{35}Cl data available for germanium(IV) compounds, studies by nuclear quadrupole resonance (NQR) exhibited quadrupolar frequencies ranging from 17.8 to 25.7 MHz, corresponding to C_Q values of approximately 35.6 to 51.4 MHz.[37] Interestingly, $CsGeCl_3$, a germanium(II) compound, has a quadrupolar frequency of 12.1 MHz, corresponding to a C_Q value of approximately 24.2 MHz.

The ^{35}Cl SSNMR spectrum of the tin cryptand complex **9** (Figure 9) was quite similar to that of the germanium(II) complexes. The signal has a similar η_Q value at 0.15 and a C_Q [^{35}Cl] value of 19 MHz, which falls well within the range determined for the germanium(II) compounds. The quadrupolar coupling constant is somewhat smaller than that observed for the cationic crown ether complex **6**. Unlike the crown ether complex, the counterion for the tin cation contains chlorine, $SnCl_3^-$. DFT calculations (*vide infra*) were, thus, required to determine whether the signal observed arose from the cation or the anion or the two signals being similar enough to be unresolvable.

DISCUSSION

Overall, the clearest trend observed is the relationship between the magnitude of the quadrupolar coupling constant and the presumed oxidation state of the attached germanium (Figure 10). Both germanium(IV) compounds exhibit *considerably* larger C_Q [^{35}Cl] values (C_Q > 40 MHz) than any of the germanium(II) compounds studied (C_Q [^{35}Cl] = 10−30 MHz). Due to the small values of η_Q observed by SSNMR spectroscopy, doubling the quadrupole frequency observed by NQR gives a reasonable approximation of the C_Q value for a compound, and thus, values obtained from NQR spectroscopy[37] are included to better illustrate the C_Q [^{35}Cl] range of germanium(IV) compounds. Out of 26 examples of germanium(IV) compounds collected by Semin *et al.*, 23 have C_Q values greater than 40 MHz, with the remaining three examples having C_Q values between 34 and 40 MHz.[37] This marked difference between the +4 and +2 oxidation states can be attributed to the covalent bond distorting the electron

dx.doi.org/10.1021/ic500728w | *Inorg. Chem.* 2014, 53, 7377−7388

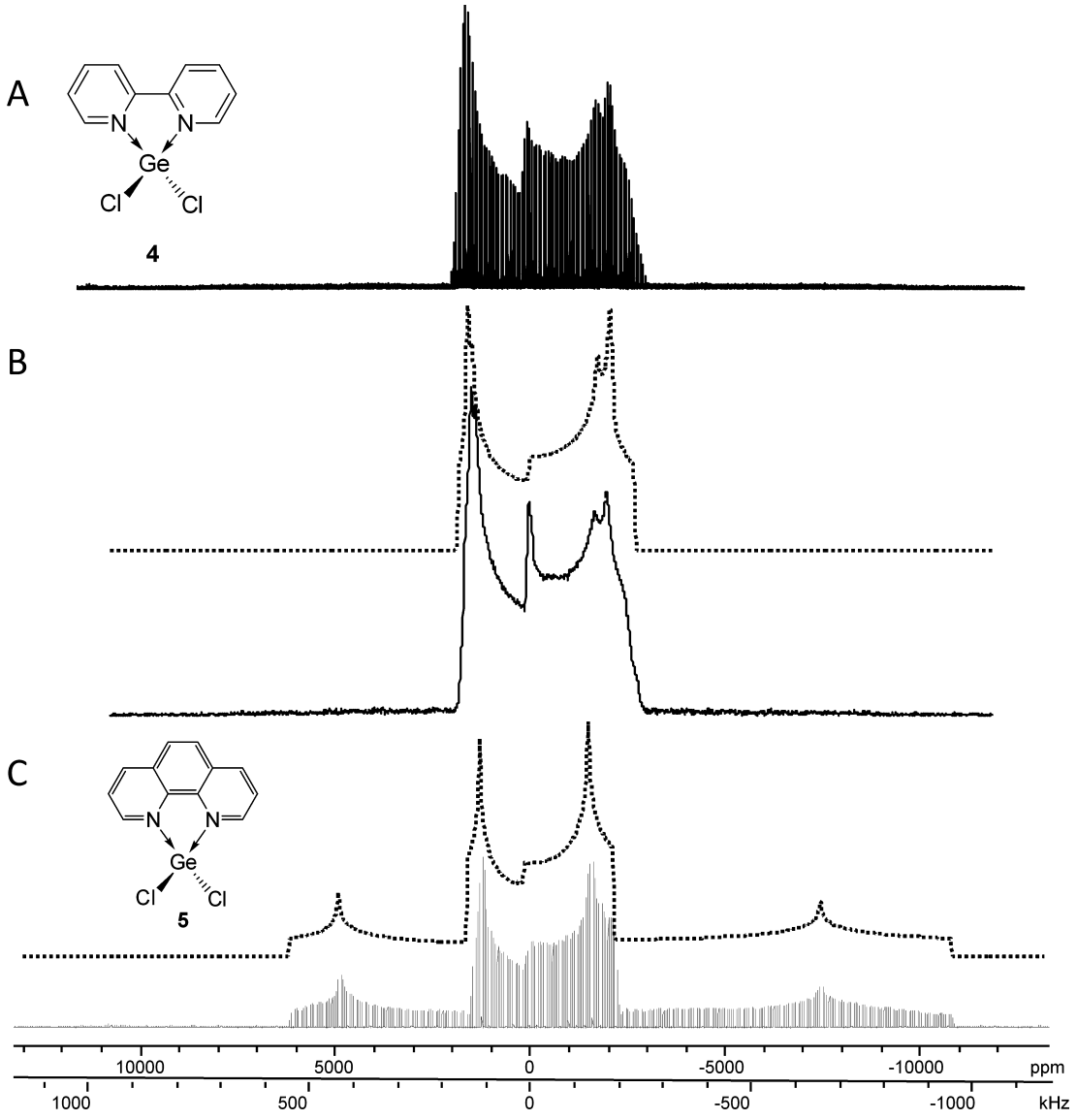

Figure 6. (A) Static ^{35}Cl WURST-QCPMG NMR spectrum of **4** at 21.1 T. (B) Static ^{35}Cl WURST-Echo NMR spectrum of **4** at 21.1 T. (C) Static ^{35}Cl WURST-QCPMG NMR spectrum of **5**. Dotted lines indicated simulated fits.

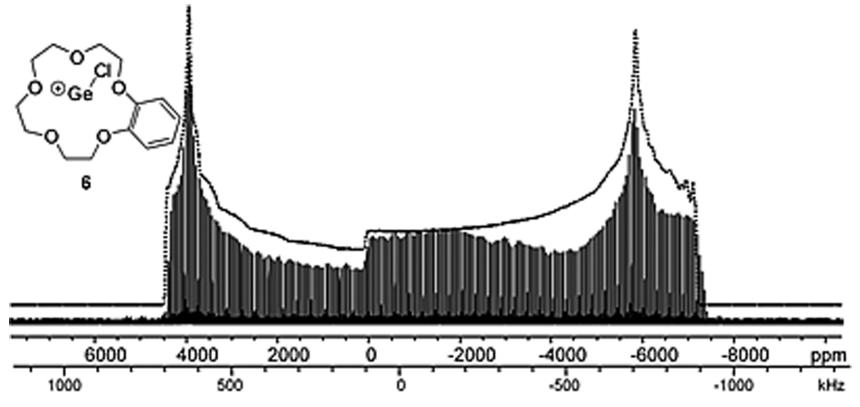

Figure 7. Static ^{35}Cl WURST-QCPMG NMR spectrum of [benzo-15-crown-5 GeCl][OTf] (**6**) at 21.1 T. The dotted trace indicates the analytical simulation.

distribution around chlorine. A higher oxidation state at germanium causes more electron density to be polarized away from chlorine, and thus, a larger electric field gradient, leading to the higher C_Q values. Larger electric field gradients in species with extensive covalent bonding are described by the Townes−Dailey theory in nuclear quadrupole resonance.[53]

The marked difference makes ^{35}Cl SSNMR spectroscopy a potentially useful tool for the assessment of oxidation states.

dx.doi.org/10.1021/ic500728w | Inorg. Chem. 2014, 53, 7377−7388

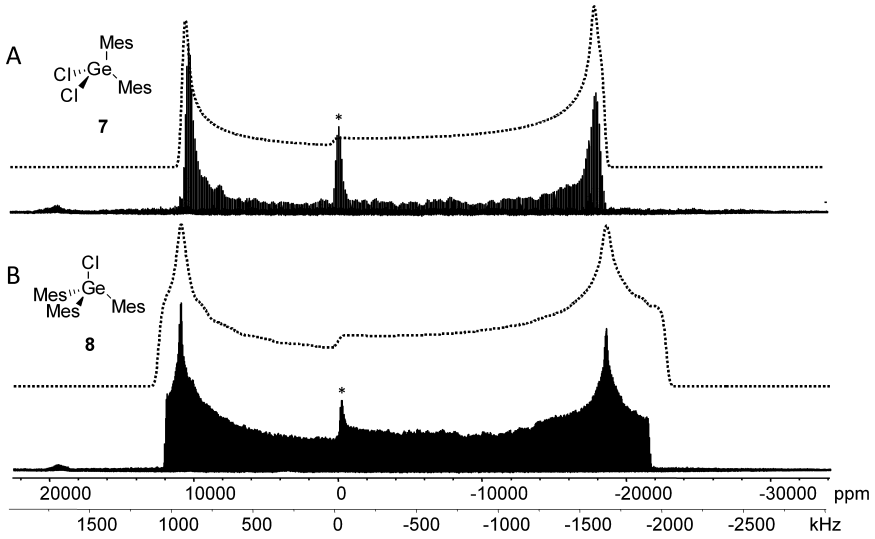

Figure 8. Static ^{35}Cl WURST-QCPMG NMR spectra of (A) **7** and (B) **8** at 21.1 T. The dotted traces indicated analytical simulations. The asterisk represents a small amount of an impurity, most likely residual $MgCl_2$ from the preparation of the germanes via a Grignard reaction.

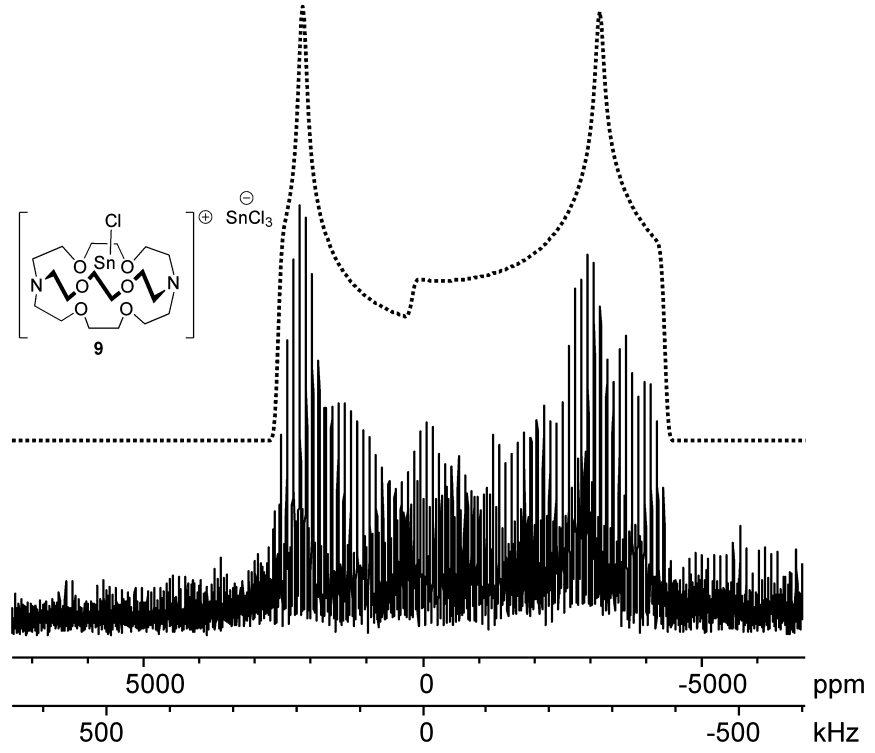

Figure 9. ^{35}Cl WURST-QCPMG NMR spectrum of [[2.2.2]cryptandSnCl][$SnCl_3$] (**9**) at 21.1 T. The dashed trace indicates the analytical simulation.

The SSNMR approach would require only that there be a chloride attached to the metalloid. This technique may complement the use of XANES, X-ray PES, and Mössbauer spectroscopy. Notably, GeCl, the only germanium(I) chloride studied by ^{35}Cl NMR spectroscopy, has an average C_Q [^{35}Cl] value of 5.5 MHz.[54] Although the C_Q [^{35}Cl] value of GeCl is larger than the value observed for uncomplexed, polymeric $GeCl_2$ (40 kHz), $GeCl_2$ is believed to have a regular octahedral environment at chlorine through self-complexation and may more closely resemble ionic compounds in structure. This suggests that while there is in general a relationship between the oxidation state of germanium and the magnitude of C_Q [^{35}Cl], there are multiple factors at play. Specifically, highly symmetrical environments at Cl will still lead to an extremely small EFG, and thus, small C_Q values. A more ionic bond will also lead to small C_Q values. Notably organic chlorides of carbon(IV)[34] also exhibit very large C_Q [^{35}Cl] values. The C_Q [^{35}Cl] values observed for the germanium(II) series are similar to those observed for transition metal metallocene complexes,[33] consistent with a less covalent bond than in organic chlorides.

Within the germanium(II) series, complexes with related ligands had similar C_Q [^{35}Cl] values. For example, the C_Q [^{35}Cl] of complexes with oxygen donors at Ge (ie **1** and **6**) fall within a 5 MHz range. The C_Q of ligands with carbon donor atoms (ie **2** and **3**) fall within an even smaller 1 MHz range. However, while three of the four signals from complexes with nitrogen donors fall

dx.doi.org/10.1021/ic500728w | Inorg. Chem. 2014, 53, 7377−7388

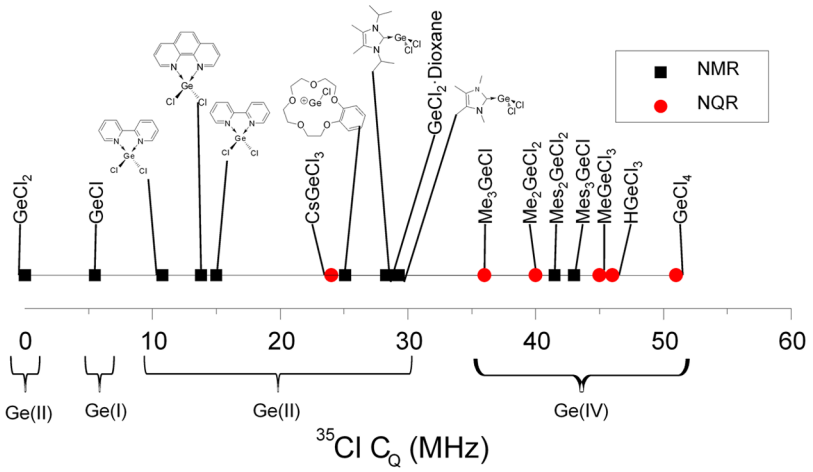

Figure 10. Relationship between ^{35}Cl quadrupolar coupling constants and the oxidation states of the attached germanium atom. Black squares indicate data obtained from NMR spectroscopy, and red circles indicate approximate C_Q values from NQR spectroscopy.[37]

within a 5 MHz range, the terminal site of complex **5** has a much larger C_Q value, suggesting that the relationship between ligands arises because similar donor strengths lead to similar Ge−Cl bond lengths rather than any direct impact of the ligand on C_Q values.

The η_Q values for **1**−**9** range from 0 for the axially symmetric Mes_3GeCl (**8**) to 0.23 for the isopropyl-substituted NHC complex of $GeCl_2$ (**3**). η_Q values of less than 0.2 generally indicate near axial symmetry at the nucleus of interest; however, it is notable that the largest η_Q values of compounds where the chlorine is bound to carbon was observed for an aryl chloride (η_Q = 0.139) despite the absence of C_3 or higher axis through the C−Cl bond.[34]

To develop solid-state NMR spectroscopy as a tool for structural characterization, it is necessary to determine if spectroscopic parameters can be correlated to structural metrics. Thus, correlations between the crystallographically determined structural metrics and the NMR spectral parameters were examined. A relationship between longer M−Cl bond lengths and smaller C_Q [^{35}Cl] value has been observed previously for the Cp_2MCl series.[33] Within the series germanium(II) complexes **1**−**6**, there was a linear relationship (R^2 = 0.90) between the inverse of the Ge−Cl bond length cubed and the magnitude of C_Q [^{35}Cl] (Figure 11A), with longer bonds leading to smaller C_Q values. If the germanium(IV) complexes are included in the fit, the trend becomes less linear (R^2 = 0.74). The trend in C_Q [^{35}Cl] values may be a consequence of the covalency of the Ge−Cl bond and may also explain the low C_Q value for GeCl, as the germanium(I) halides are not expected to have traditional covalent bonds.[54] Likewise, the high symmetry in $GeCl_2$ may arise from the Ge−Cl bonds having low covalent character.[35] Indeed, Natural Bond Order calculations on complexes **1**−**6** at the TPSSTPSS/6-311+G** level revealed Ge−Cl bond orders well below the value of 1 expected for a traditional covalent bond. While the germanium(IV) compounds are predicted to have shorter Ge−Cl bonds from the geometry-optimized structures, the experimental C_Q [^{35}Cl] values fall well above those predicted by extrapolation of the trend observed for the germanium(II) compounds. Apparently, the distortion of the electron distribution around chlorine resulting from proximity to germanium is greater when there is a higher germanium oxidation state. The experimental C_Q value for **9** also does not follow the exact trend

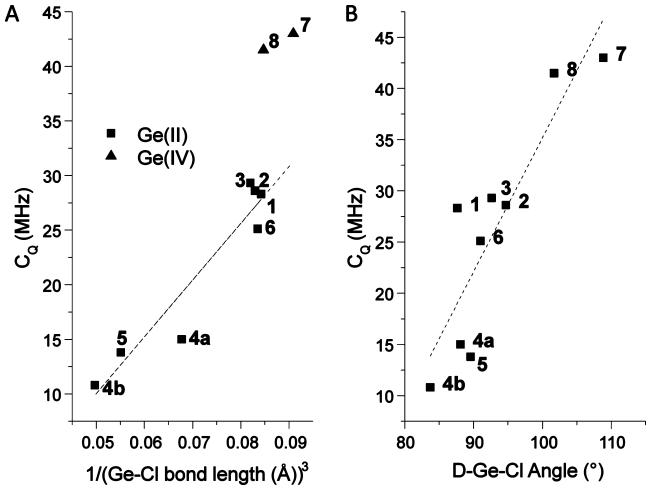

Figure 11. (A) Relationship between experimental ^{35}Cl quadrupolar coupling constant and crystallographically determined Ge−Cl bond lengths. The dashed line indicates a line of best fit for the germanium(II) compounds indicated by the solid squares (y = 519x − 16, R^2 = 0.90). The germanium(IV) compounds are indicated by solid triangles. (B) Relationship between ^{35}Cl quadrupolar coupling constant and Donor−Ge−Cl angle. Angles were determined crystallographically for **1**−**6** and from geometry optimized structures for **7** and **8**. The dashed line indicates a line of best fit (y = 1.31x − 95.6, R^2 = 0.76).

due to the difference in electronegativity between germanium and tin.

The average angle between chlorine, germanium, and the donor atom correlated weakly to C_Q (Figure 11B), with wider bond angles corresponding to larger C_Q values in a linear manner (R^2 = 0.76). If the covalently bound substituents are regarded as being donors, the germanium(IV) compounds **7** and **8** fit the trend of wide angles corresponding to large C_Q values (using the geometry-optimized structures).

Computational Investigations. Theoretical calculations are increasingly used as a complement to SSNMR spectroscopy. In complexes **4**, **5**, and **9**, where two distinct chloride sites exist, calculations are the only way to assign the observed signal(s) by comparison of the experimental to the predicted parameters. The calculation of SSNMR parameters also makes it possible to determine the orientations of the individual tensor components, which can then be used to rationalize the trends observed

dx.doi.org/10.1021/ic500728w | Inorg. Chem. 2014, 53, 7377−7388

Table 2. Summary of Computational ^{35}Cl NMR Parameters of Compounds 1−9[a] Calculated Using Gaussian 09

compound	donor atom	calculated C_Q (MHz)	exptl. C_Q (MHz)	calculated η_Q	exptl. η_Q	calculated Ω (ppm)	calculated κ
1[b]	O	28.5	28.3	0.12	0.055		
2[b]	C	33.2	29.3	0.10	0.12	300	−0.7
3	C	34.0	28.6	0.04	0.23	350	−0.6
4[b] Cl(1)	N	23.6	15.3	0.25	0.13	500	0.6
4[b] Cl(2)	N	14.8	14.1	0.2	0.1	600	0.4
5[b] Cl(1)	N	18.0	13.8	0.10	0.15	400	0.04
5[b] Cl(2)	N	34.7	29.6	0.18	0.18	420	0.9
6	O	27.8	25.1	0.10	0.1	550	0.6
7	C	44.5	43.0	0.13	0.1	310	0.5
8	C	43.3	41.5	0	0	120	1
9	O, N	22.7	19.0	0.13	0.15	1103	−0.2

[a]Hydrogen positions for **2**−**6** and **9** were optimized using the TPSSTPSS/6-31G* method. Structures for **7** and **8** were fully optimized at the TPSSTPSS/6-31G* level. [b]Calculations included long-range interactions with the adjacent $GeCl_2$ unit.

experimentally. Finally, the accurate calculation of NMR parameters can offer support for a geometry-optimized structure when there is not an X-ray structure available.

Previous calculations of ^{35}Cl SSNMR parameters have been performed using plane wave pseudopotentials using CASTEP.[33,50,55] The CASTEP code is optimized for calculations on periodic inorganic solids.[56] Calculations model electron distribution throughout the entire unit cell, and thus, require extensive computational resources for substances with large unit cells. Of the compounds included in this study, only $GeCl_2$·dioxane (**1**) had a unit cell small enough for CASTEP calculations. The other complexes crystallized in unit cells which were too large (>1000 Å^3) to model in CASTEP with the available computational resources. The experimental ^{35}Cl SSNMR parameter (η_Q and C_Q) values of organic chlorides[34] and trimethylammonium chloride[57] have been reasonably reproduced using DFT calculations at the B3LYP/6-311+G** level of theory on isolated molecules using the solid-state geometry as determined by X-ray diffraction. As the complexes in this study are molecular solids, *Gaussian 09* calculations also appeared appropriate. No thorough investigation of *Gaussian* methodology for the calculation of ^{35}Cl SSNMR parameters has been undertaken to date. Model chemistries were assessed using $GeCl_2$·dioxane (**1**) as it was possible to calculate NMR parameters for this complex using CASTEP, giving a point of comparison to established methodology. A thorough discussion of the assessment can be found in the Supporting Information.

A summary of the computational results is presented in Table 2. As the TPSSTPSS/6-311+G** methodology proved to be the most accurate and efficient for $GeCl_2$·dioxane (**1**), it was employed for all subsequent calculations of ^{35}Cl NMR parameters. Hydrogen positions were optimized at the TPSSTPSS/6-31G* level. The ^{35}Cl CSA interaction was overestimated in all cases, ranging from 300 to 600 ppm while the experimental values ranged from 200 to 350. However, the experimental values have large errors due to the large effect of EFG on line shape compared to CSA and CSA only being observable at one field.

The ^{35}Cl NMR parameters for the methyl-substituted NHC·$GeCl_2$ complex **2** were calculated for both the isolated molecule and the dimeric structure apparent from the X-ray data.[43] Calculation on the monomer gave a C_Q [^{35}Cl] value of 34.6 MHz. Inclusion of the pseudobridging interaction with the adjacent molecule offered a modest improvement in agreement with a calculated C_Q value of 33.2 MHz. The small value of η_Q was in reasonable agreement. The similarity between the calculated C_Q values for both the monomeric and dimeric structures suggests that the pseudobridging $Ge_{(adjacent)}$−Cl interaction is not as important for complex **2** as it is for $GeCl_2$·dioxane, for which the difference between the monomeric and cluster structures was dramatic. A similar C_Q value (34 MHz) was calculated for the monomeric isopropyl-substituted NHC·$GeCl_2$ complex **3**. Combined with the similar experimental C_Q values for **2** and **3**, the computational results support that the long-range pseudobridging Ge−Cl interaction is not as important in the carbene complexes as it is for **1**. This is most likely due to the adjacent germanium atom being 0.27 Å closer to the pseudobridging chloride in **1** than in **2**, which may in turn arise from the NHC being a better electron donor than dioxane in addition to being more sterically demanding.

While the intermolecular interactions proved to be less important for accurate reproduction of the parameters for **2** and **3** than for $GeCl_2$·dioxane, the interactions were still potentially important, and thus, calculations on the bipyridine complex **4** included the adjacent molecules to either side of the chloride of interest. The quadrupolar coupling constants were overestimated at 23.6 MHz for Cl(1) and 14.8 MHz for Cl(2). The Ge−Cl(2) bond length (2.7195 Å) is considerably longer than a typical covalent Ge−Cl bond. Indeed, in the related bromine complex, one of the analogous bromides is fully anionic in character.[7f] A longer covalent bond would have a less dramatic effect on the electric field gradient, leading to a lower C_Q value. The relative ordering is also consistent with the general trend observed experimentally (Figure 11). Calculations predict similar η_Q values for both chlorine sites of roughly 0.2, which is within experimental error of the experimental values of 0.13 and 0.1. The phenanthroline complex **5** was much less ambiguous with calculated C_Q [^{35}Cl] values of 18 MHz for the pseudobridging chloride and 34.7 MHz for the terminal chlorine. The calculated values again somewhat overestimated C_Q while accurately reproducing the small η_Q values.

The C_Q [^{35}Cl] value for the crown ether GeCl complex **6** was slightly overestimated at 27.8 MHz. A difference of 2 MHz, while greater than the experimental error, is still reasonable for such a large C_Q value. The value of η_Q was reasonably reproduced.

While there are no X-ray structures available for the two germanium(IV) compounds **7** and **8**, calculations were performed using structures optimized at the TPSSTPSS/6-31G* level. Gaussian calculations on compound **7** predicted a C_Q [^{35}Cl] of 44.5 MHz and η_Q of 0.13. A difference of 1.5 MHz from the experimental C_Q value of 43.0 MHz is very reasonable agreement for such a broad signal. Compound **8** demonstrated a

dx.doi.org/10.1021/ic500728w | Inorg. Chem. 2014, 53, 7377−7388

similar agreement, with a calculated C_Q value of 43.3 MHz, overestimating the value of C_Q to the same degree as in **7**, and an η_Q value of 0, exactly in agreement with experimental results.

For **9**, the LAN2DZ basis set was employed for tin, as the 6-311+G** basis set does not include fourth row elements. All other elements in the structure were calculated using the latter basis set. Much like **4** and **5**, DFT calculations were required to determine why only one chlorine signal was observed when there are two distinct chloride environments in **9**. The chloride bound to the cationic tin site was predicted to have a C_Q [^{35}Cl] value of 22.7 MHz, in reasonable agreement with the 19 MHz observed experimentally. The chlorides of the $SnCl_3^-$ counteranion have a calculated C_Q [^{35}Cl] value of 105 MHz, confirming that the signal observed is most reasonably assigned to the cationic site. Even considering the trend toward overestimating C_Q in the DFT calculations, the anionic chlorides would be over 10 MHz broad at 21.1 T, and thus, are not observed.

The overall agreement between the calculated and experimental C_Q[^{35}Cl] values is illustrated in Figure 12. Overall, the correlation between the experimental values is linear, with an R^2 value of 0.93. With an ideal 1:1 correlation, the slope of the line of best fit would be 1; it is instead 0.92, suggesting that the overall agreement between theory and experiment is reasonable. The C_Q values of the germanium(IV) compounds **8** and **9** were reasonably reproduced using geometry-optimized structures.

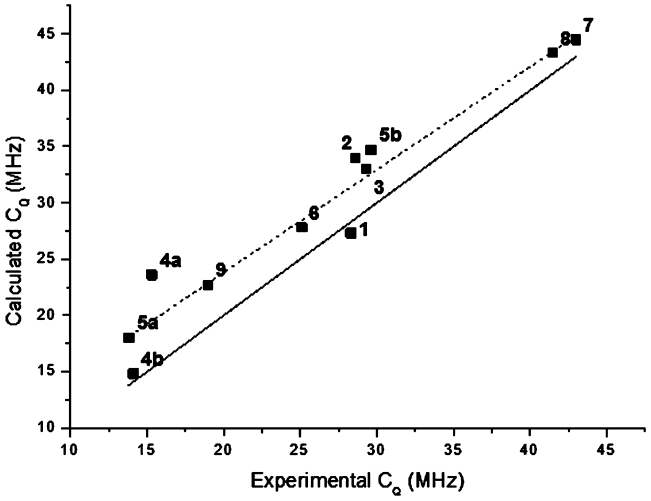

Figure 12. Agreement between calculated and experimental C_Q [^{35}Cl] values. The solid line represents an ideal 1:1 correlation, while the dashed line represents a line of best fit ($y = 0.92x + 5.5$, $R^2 = 0.93$).

The orientation of the EFG tensor components (Figure S5) can often provide insight into the specific structural effects on the NMR parameters. In the majority of the germanium(II) complexes, the largest tensor component (V_{33}) was oriented along the Ge−Cl bond, with the remaining components oriented perpendicular, explaining the general relationship observed between the Ge−Cl bond length and the magnitude of C_Q.

The V_{22} and V_{11} components of **2**−**6** are not orientated toward any particular structural feature, providing a possible explanation for the similar η_Q values observed for all compounds. Notably, the situation is somewhat different for $GeCl_2$·dioxane (**1**), with the intermediate component (V_{22}) being oriented along the Ge−Cl bond and the largest component (V_{33}) being oriented toward the adjacent germanium atom. This was not seen in any of the other complexes which feature a long-range Ge−Cl contact (**2**, **4**, and **5**), offering a possible explanation for why $GeCl_2$·dioxane is an outlier in the structural trend relating C_Q to bond angle (Figure 11). The greater influence of the long-range contact may be attributed to the adjacent germanium atom being 0.2 Å closer in $GeCl_2$·dioxane than in **4**, with **5** having an even more distant contact.

The same tensor orientation pattern is observed in germanium(IV) compounds (Figure S6). While the geometry-optimized Ge−Cl bond lengths (2.224 Å for Mes_2GeCl_2 and 2.277 Å for Mes_3GeCl) are the shortest Ge−Cl bond lengths in this study, the bond lengths are not sufficiently different from those of the germanium(II) complexes to reasonably be the only explanation for the dramatic difference observed in C_Q values. The oxidation state at germanium, thus, appears to be the most important influence on the value of C_Q; however it is likely that bond length will play a role in determining the magnitude of C_Q [^{35}Cl] within the subcategory of germanium(IV) compounds

Finally, the same tensor orientation pattern, with the V_{33} component aligned with the element−Cl bond, is also observed for the tin complex **9** (Figure S6). While this is a single example, it points to the possibility that the same trends might be observed for other group 14 compounds.

CONCLUSIONS

All the compounds examined in this study gave rise to broad ^{35}Cl solid-state NMR spectra as is expected for terminal, covalently bound chlorides. Through the use of the WURST-QCPMG pulse sequence and piecewise acquisition, it was possible to obtain spectra suitable for extraction of quadrupolar parameters through spectral simulation. This is in marked contrast to attempts to obtain ^{73}Ge SSNMR spectra for the same compounds. While ^{73}Ge NMR spectroscopy was attempted for the majority of the selected compounds, it was only possible to obtain a reasonable ^{73}Ge SSNMR spectrum for $GeCl_2$·dioxane, which, nonetheless, still required 1 week of acquisition time at 21.1 T.[48]

Examination of the ^{35}Cl parameters revealed apparent relationships to several properties of germanium including the Ge−Cl bond length and the donor−Ge−Cl bond angle which can provide insights into the coordination environment about germanium. However, the most dramatic observation is the distinct relationship between the assigned oxidation state of germanium and the ^{35}Cl quadrupolar coupling constant. Germanium(IV) compounds exhibit considerably broader (C_Q [^{35}Cl] > 40 MHz) signals than germanium(II) compounds (C_Q [^{35}Cl] = 10−30 MHz), providing a possible indicator of oxidation state at germanium. Indeed, the difference in the magnitudes of the C_Q [^{35}Cl] exceeded that which could be accounted for by the tendency of germanium(IV) compounds to have shorter Ge−Cl bonds. If the observed correlation persists in additional samples, ^{35}Cl SSNMR spectroscopy could prove to be a more accessible alternative to synchrotron techniques for assessing oxidation states of main group chlorides. In tin chemistry, oxidation states are often determined by Mössbauer spectroscopy; however, there is no appropriate gamma ray source for the Mössbauer spectroscopy of germanium compounds, adding to the value of the oxidation state information available from ^{35}Cl SSNMR spectroscopy. A comparative study of the oxidation states of tin determined by Mössbauer spectroscopy and by ^{35}Cl SSNMR spectroscopy may provide an independent and experimentally based validation for the hypothesized connection between quadrupolar coupling data and oxidation state.[58]

dx.doi.org/10.1021/ic500728w | Inorg. Chem. 2014, 53, 7377−7388

In the extreme, when the distortion of the electron density results in an ionic bond, the magnitudes of the C_Q [^{35}Cl] can be smaller than predicted based on oxidation states. Indeed, the ^{35}Cl SSNMR data reported focuses on ionic inorganic chlorides,[24] which have considerably narrower spectra than covalent organic chlorides.[34] Symmetry at chlorine will also influence the magnitude of C_Q. Nonetheless, the observed correlation is notable, and further studies are required to determine and understand the factors influencing the magnitude of C_Q [^{35}Cl] in main group chlorides.

Within the series of germanium(II) complexes studied, ligands with common donor atoms gave rise to signals with similar C_Q [^{35}Cl] values, most likely due to the similar electronic environment at germanium. The largest EFG tensor component of the majority of the germanium(II) complexes was oriented along the Ge−Cl bond, as determined by TPSSTPSS/6-311+G** model chemistry. This suggests that the general relationship noted between the donor atom and the value of C_Q [^{35}Cl] is likely due to similar germanium chlorine bond lengths due to comparable structures. $GeCl_2$·dioxane is a notable exception as the V_{33} component is, instead, oriented toward the adjacent germanium atom, which explains why the pseudobridging Ge−Cl interaction (which is the closest such interaction seen in this study) has the largest influence on C_Q. The V_{33} tensor orientation for the germanium(IV) compounds (**7** and **8**) was also along the Ge−Cl bond, suggesting that there may be a similar relationship between C_Q [^{35}Cl] and Ge(IV)−Cl bond length. Finally, the cationic tin complex also has an EFG tensor with the largest component oriented along the E−Cl bond, leading to the possibility of extending this study into the rest of the group 14 elements.

EXPERIMENTAL SECTION

Materials. $GeCl_2$·dioxane (**1**),[40] **2**,[43] **3**,[44] **4**,[7f] **5**,[7f] **6**,[45] Mes_2GeCl_2 (**7**),[59] Mes_3GeCl (**8**),[59] and **9**[47] were all prepared according to literature procedures. The identities of the compounds were confirmed by solution state ^{1}H NMR spectroscopy.

Solid-State NMR Spectroscopy. ^{35}Cl SSNMR spectra were acquired on a Bruker Avance 900 MHz spectrometer at the *National Ultrahigh Field NMR Facility for Solids* (http://nmr900.ca). ^{35}Cl experimental setup and pulse calibrations were performed on 1 M KCl in H_2O, and chemical shift referencing was performed relative to this sample. Spectra were acquired under static conditions on a dual channel H/X 7 mm low gamma probe with high power ^{1}H decoupling. With the exception of the spectrum of **1** shown in Figure 4A, which was acquired using the QCPMG[25] pulse sequence, and the spectrum of **4** shown in Figure 6B, which was acquired using a WURST-echo sequence, all spectra were acquired using a WURST-QCPMG[29] sequence with a 50 μs WURST-80 pulse for both excitation and refocusing and τ_1 = 25 μs, $\tau_2 = \tau_3 = \tau_4 = 26$ μs. Specific acquisition parameters for individual compounds are given in Table S2.

Low field data were acquired on a Varian Infinity 400 spectrometer. The WURST-QCPMG experimental setup was performed on solid $CaCl_2$·$2H_2O$ and chemical shift referencing was performed relative to solid KCl (8.5 ppm relative to 0.1 M NaCl in H_2O at 0 ppm). Spectra were acquired in a piecewise manner with a 150 kHz offset between subspectra. A 50 μs WURST-80 pulse was used for both excitation and refocusing.

NMR Spectral Simulations. Experimental NMR parameters were determined from analytical simulations using WSolids.[60] Errors were determined by visual comparison to the experimental spectrum. Starting from the best fit value, the parameter being evaluated was varied systematically in both directions while all others were held constant until a visible change was observed.

Theoretical Calculations. First-principles calculations were performed using Gaussian 09[61] on the Shared Hierarchical Academic Research Computing Network (SHARCNET, www.sharcnet.ca). Calculations were performed on a four core Opteron 2.4 GHz CPU with 32 GB of memory or an eight core Xeon 2.83 GHz CPU with 16 GB of memory. CSA tensors were computed using the gauge-including atomic orbitals (GIAO) method. For structures with available X-ray structures, atomic coordinates were taken directly from the CIF file and hydrogen positions optimized at the TPSSTPSS/6-31G* level. The compounds without available crystal structures were fully geometry-optimized at the same level. Basis sets and methods were used as indicated. The results of the Gaussian calculations were analyzed using EFGShield.[62]

ASSOCIATED CONTENT

Supporting Information

Six figures, two tables and optimization of computational methodology. This material is available free of charge via the Internet at http://pubs.acs.org.

AUTHOR INFORMATION

Corresponding Author

*E-mail: kbaines2@uwo.ca.

*E-mail: yhuang@uwo.ca.

Notes

The authors declare no competing financial interest.

ACKNOWLEDGMENTS

Access to the 900 MHz NMR spectrometer was provided by the *National Ultrahigh-Field NMR Facility for Solids* (Ottawa, Canada), a national research facility funded by the Canada Foundation for Innovation, the Ontario Innovation Trust, Recherche Québec, the National Research Council Canada, and Bruker BioSpin and managed by the University of Ottawa. Computational work was made possible by the facilities of the Shared Hierarchical Academic Research Computing Network (SHARCNET: www.sharcnet.ca) and Compute/Calcul Canada. We thank Prof. Robert Schurko (University of Windsor) for providing the WURST-QCPMG pulse sequence. The Natural Sciences and Engineering Research Council of Canada (NSERC) is acknowledged for a Major Resources Support grant as well as Discovery Grants to Y.H. and K.M.B. Y.H. also thanks NSERC for a Discovery Accelerator Grant and the Canada Research Chair program for funding. We thank Teck Metals Ltd. for a generous donation of $GeCl_4$. $GeCl_2$·dioxane (**1**) was prepared by Paul A. Rupar. Compound **9** was prepared by Jessica C. Avery.

REFERENCES

(1) Parkin, G. *J. Chem. Educ.* **2006**, *83*, 791. We note that the oxidation state is the same as the valence of germanium in the complexes studied in this paper.

(2) Rivard, E.; Power, P. P. *Dalton Trans.* **2008**, 4336.

(3) Mandal, S. K.; Roesky, H. W. *Chem. Commun.* **2010**, *46*, 6016.

(4) Lee, V. Ya.; Sekiguchi, A. In *Organometallic Compounds of Low-Coordinate Si, Ge, Sn and Pb: From Phantom Species to Stable Compounds*; Wiley: Chichester, U. K., 2010.

(5) Asay, M.; Jones, C.; Driess, M. *Chem. Rev.* **2011**, *111*, 354.

(6) Levason, W.; Reid, G.; Zhang, W. *Coord. Chem. Rev.* **2011**, *255*, 1319.

(7) For selected examples, see: (a) Al-Rafia, S. M. I.; Momeni, M. R.; McDonald, R.; Ferguson, M. J.; Brown, A.; Rivard, E. *Angew. Chem., Int. Ed.* **2013**, *52*, 6390. (b) Xion, Y.; Yao, S.; Tan, G.; Inoue, S.; Driess, M. *J. Am. Chem. Soc.* **2013**, *135*, 5004. (c) Xion, Y.; Yao, S.; Inoue, S.; Berkefeld, A.; Driess, M. *Chem. Commun.* **2012**, *48*, 12198. (d) Singh, A. P.; Roesky, H. W.; Carl, E.; Stalke, D.; Demers, J.-P.; Lange, A. *J. Am. Chem. Soc.* **2012**, *134*, 4998. (e) Li, J.; Stasch, A.; Schenk, C.; Jones, C. *Dalton Trans.* **2011**, *40*, 10448. (f) Cheng, F.; Dyke, J. M.; Ferrante, F.;

Hector, A. L.; Levason, W.; Reid, G.; Webster, M.; Zhang, W. *Dalton Trans.* **2010**, *39*, 847. (g) Rupar, P. A.; Jennings, M. C.; Baines, K. M. *Organometallics* **2008**, *27*, 5043. (h) Ding, Y.; Hao, H.; Roesky, H. W.; Noltemeyer, H.; Schmidt, H.-G. *Organometallics* **2001**, *20*, 4806. (i) Probst, T.; Steigelmann, O.; Riede, J.; Schmidbaur, H. *Angew. Chem., Int. Ed. Engl.* **1990**, *12*, 1397.
(8) (a) Mirzadeh, N.; Bennett, M.; Wagler, J.; Wächtler, E.; Gerke, B.; Pöttgen, R.; Bhargava. *Eur. J. Inorg. Chem.* **2013**, 1997. (b) Brendler, E.; Wächtler, E.; Heine, T.; Zhechkov, L.; Langer, T.; Pöttgen, R.; Hill, A. F.; Wagler, J. *Angew. Chem., Int. Ed.* **2011**, *50*, 4696.
(9) Bancroft, G. M. *Mössbauer Spectroscopy: An Introduction for Inorganic Chemists and Geochemists*; Wiley: New York, 1973.
(10) Shimizu, K.; Kamiya, Y.; Osaki, K.; Yoshida, H.; Satsuma, A. *Catal. Sci. Technol.* **2012**, *2*, 767.
(11) Ward, M. J.; Rupar, P. A.; Murphy, M. W.; Yiu, Y.; Baines, K. M.; Sham, T. K. *Chem. Commun.* **2010**, *46*, 7016.
(12) Brouwer, D. H. In *NMR Crystallography*; Harris, R. K., Wasylishen, R. E., Duer, M. J., Eds.; John Wiley & Sons: Chichester, U. K., 2009; p 263.
(13) Lo, A. Y. H.; Bitterwolf, T. E.; Macdonald, C. L. B.; Schurko, R. W. *J. Phys. Chem. A* **2005**, *109*, 7073.
(14) Papulovskiy, E.; Shubin, A. A.; Terskikh, V. V.; Pickard, C. J.; Lapina, O. B. *Phys. Chem. Chem. Phys.* **2013**, *15*, 5115.
(15) Alov, N. *J. Anal. Chem.* **2005**, *60*, 432.
(16) Pykko, P. *Mol. Phys.* **2008**, *106*, 1965.
(17) Takeuchi, Y.; Takayama, T. *Annu. Rep. NMR Spectrosc.* **2005**, *54*, 155.
(18) Perras, F. A.; Viger-Gravel, J.; Burgess, K. M. N.; Bryce, D. L. *Solid State Nucl. Magn. Reson.* **2013**, *51*−*52*, 1.
(19) Michaelis, V. K.; Kroeker, S. *J. Phys. Chem. C* **2010**, *114*, 21736.
(20) Hanson, M. A. Structural Elucidation of Group 14 Compounds by Solid-State NMR Spectroscopy. Ph. D. Thesis, The University of Western Ontario, London, ON, Canada, 2012.
(21) Weinert, C. S. *ISRN Spectrosc.* **2012**, *2012*, 1.
(22) Brown, T. H.; Green, P. J. *J. Am. Chem. Soc.* **1970**, *92*, 2359.
(23) Chen, F.; Ma, G.; Bernard, G. M.; Wasylishen, R. E.; Cavell, R. G.; McDonald, R.; Ferguson, M. J. *Chem.—Eur. J.* **2013**, *19*, 2826.
(24) Widdifield, C. M.; Chapman, R. P.; Bryce, D. L. *Annu. Rep. NMR Spectrosc.* **2009**, *66*, 195.
(25) Larsen, F. H.; Jakobsen, H. J.; Ellis, P. D.; Nielsen, N. C. *J. Phys. Chem. A* **1997**, *101*, 8597.
(26) Schurko, R. W.; Hung, I.; Widdifield, C. M. *Chem. Phys. Lett.* **2003**, *379*, 1.
(27) O'Dell, L. A.; Rossini, A. J.; Schurko, R. W. *Chem. Phys. Lett.* **2009**, *468*, 330.
(28) Siegel, R.; Nakashima, T. T.; Wasylishen, R. E. *J. Magn. Reson.* **2007**, *184*, 85.
(29) O'Dell, L. A.; Schurko, R. W. *Chem. Phys. Lett.* **2008**, *464*, 97.
(30) MacKenzie, K. J. D.; Smith, M. E. In *Multinuclear Solid-State NMR of Inorganic Materials*; 1st ed.; Pergamon: New York, 2002; p 461.
(31) Bryce, D. L.; Sward, G. D. *Magn. Reson. Chem.* **2006**, *44*, 409.
(32) Butler, B. J.; Hook, J. M.; Harper, J. B. *Annu. Rep. NMR Spectrosc.* **2011**, *73*, 63.
(33) Rossini, A. J.; Mills, R. W.; Briscoe, G. A.; Norton, E. L.; Geier, S. J.; Hung, I.; Zheng, S.; Autschbach, J.; Schurko, R. W. *J. Am. Chem. Soc.* **2009**, *131*, 3317.
(34) Perras, F. A.; Bryce, D. L. *Angew. Chem., Int. Ed.* **2012**, *51*, 4227.
(35) Greer, B. J.; Michaelis, V. K.; Terskikh, V. V.; Kroeker, S. *Can. J. Chem.* **2011**, *89*, 1118.
(36) Rouse, R. C.; Peacor, D. R.; Maxim, B. R. *Z. Kristallogr.* **1977**, *145*, 161.
(37) Semin, G. K.; Babushkina, T. A.; Yakobson, G. G. In *Nuclear Quadrupole Resonance in Chemistry*; Keter Publishing House: Jerualem, Israel, 1975; p 285.
(38) Hadipour, N. L.; Rafice, M. A.; Javaheri, M.; Mousavie, M. *Chem. Phys. Lett.* **2002**, *356*, 445.
(39) Khulishov, V. I.; Bokii, N. G.; Struchkov, Y. T.; Nefedov, O. M.; Kolesnikov, S. P.; Perl'mutter, B. M. *Zh. Strukt. Khim.* **1970**, *11*, 71.
(40) Leigh, W. J.; Harrington, C. R.; Vargas-Baca, I. *J. Am. Chem. Soc.* **2004**, *126*, 16105.
(41) Denk, M. K.; Khan, M.; Lough, A. J.; Shuchi, K. *Acta Crystallogr., Sect. C* **1998**, *C54*, 1830.
(42) Baines, K. M.; Stibbs, W. G. *Coord. Chem. Rev.* **1995**, *145*, 157.
(43) Ruddy, A. J.; Rupar, P. A.; Bladek, K. J.; Allan, C. J.; Avery, J. C.; Baines, K. M. *Organometallics* **2010**, *29*, 1362.
(44) Rupar, P. A.; Staroverov, V. N.; Ragogna, P. J.; Baines, K. M. *J. Am. Chem. Soc.* **2007**, *129*, 15138.
(45) Rupar, P. A.; Bandyopadhyay, R.; Cooper, B. F. T.; Stinchcombe, M. R.; Ragogna, P. J.; Macdonald, C. L. B.; Baines, K. M. *Angew. Chem., Int. Ed.* **2009**, *48*, 5155.
(46) Cheng, F.; Hector, A. L.; Levason, W.; Reid, G.; Webster, M.; Zhang, W. *Angew. Chem., Int. Ed.* **2009**, *48*, 5152.
(47) Avery, J. C.; Hanson, M. A.; Herber, R. H.; Bladek, K. J.; Rupar, P. A.; Nowik, I.; Huang, Y.; Baines, K. M. *Inorg. Chem.* **2012**, *51*, 7306.
(48) Sutrisno, A.; Hanson, M. A.; Rupar, P. A.; Terskikh, V. V.; Baines, K. M.; Huang, Y. *Chem. Commun.* **2010**, *46*, 2817.
(49) Chapman, R. P.; Bryce, D. L. *Phys. Chem. Chem. Phys.* **2009**, *11*, 6987.
(50) Bryce, D. L.; Bultz, E. B. *Chem.—Eur. J.* **2007**, *13*, 4786.
(51) Lucier, B. E. G.; Johnston, K. E.; Xu, W.; Hanson, J. C.; Senanayake, S. D.; Yao, S.; Bourassa, M. W.; Srebro, M.; Autschbach, J.; Schurko, R. W. *J. Am. Chem. Soc.* **2014**, *136*, 1333.
(52) Chapman, R. P.; Widdifield, C. M.; Bryce, D. L. *Prog. Nucl. Magn. Reson. Spectrosc.* **2009**, *55*, 215.
(53) Townes, C. H.; Dailey, B. P. *J. Chem. Phys.* **1949**, *17*, 782.
(54) Hanson, M. A.; Schnepf, A.; Terskikh, V. V.; Huang, Y.; Baines, K. M. *Aust. J. Chem.* **2013**, *66*, 1202.
(55) Chapman, R. P.; Bryce, D. L. *Phys. Chem. Chem. Phys.* **2007**, *9*, 6219.
(56) Segall, M. D.; Lindan, P. J. D.; Probert, M. J.; Pickard, C. J.; Hasnip, P. J.; Clark, S. J.; Payne, M. C. *J. Phys.: Condens. Matter* **2002**, *14*, 2717.
(57) Penner, G. H.; Webber, R.; O'Dell, L. A. *Can. J. Chem.* **2011**, *89*, 1036.
(58) We thank a reviewer for this suggestion.
(59) Cooke, J. A.; Dixon, C. E.; Netherton, M. R.; Kollegger, G. M.; Baines, K. M. *Synth. React. Inorg. Met.−Org. Chem.* **1996**, *26*, 1205.
(60) Eichele, K.; Wasylishen, R. E. In *WSolids1: Solid-State NMR Spectrum Simulation*, 2001.
(61) Frisch, M. J.; Trucks, G. W.; Schlegel, H. B.; Scuseria, G. E.; Robb, M. A.; Cheeseman, J. R.; Scalmani, G.; Barone, V.; Mennucci, B.; Petersson, G. A.; Nakatsuji, H.; Caricato, M.; Li, X.; Hratchian, H. P.; Izmaylov, A. F.; Bloino, J.; Zheng, G.; Sonnenberg, J. L.; Hada, M.; Ehara, M.; Toyota, K.; Fukuda, R.; Hasegawa, J.; Ishida, M.; Nakajima, T.; Honda, Y.; Kitao, O.; Nakai, H.; Vreven, T.; Montgomery, J. A., Jr.; Peralta, J. E.; Ogliaro, F.; Bearpark, M.; Heyd, J. J.; Brothers, E.; Kudin, K. N.; Staroverov, V. N.; Kobayashi, R.; Normand, J.; Raghavachari, K.; Rendell, A.; Burant, J. C.; Iyengar, S. S.; Tomasi, J.; Cossi, M.; Rega, N.; Millam, N. J.; Klene, M.; Knox, J. E.; Cross, J. B.; Bakken, V.; Adamo, C.; Jaramillo, J.; Gomperts, R.; Stratmann, R. E.; Yazyev, O.; Austin, A. J.; Cammi, R.; Pomelli, C.; Ochterski, J. W.; Martin, R. L.; Morokuma, K.; Zakrzewski, V. G.; Voth, G. A.; Salvador, P.; Dannenberg, J. J.; Dapprich, S.; Daniels, A. D.; Farkas, Ö.; Foresman, J. B.; Ortiz, J. V.; Cioslowski, J.; Fox, D. J. *Gaussian 09*, revision A1 ed.; Gaussian Inc.: Wallingford, CT, 2009.
(62) Adiga, S.; Aebi, D.; Bryce, D. L. *Can. J. Chem.* **2007**, *85*, 496.